

Original Article

A Learning on Intensity Prediction of Tropical Cyclone Infrared Images by Gabor Filter on Binary and Multi Class Approach

S. Jayasree¹, K.R. Ananthapadmanaban²

^{1,2}Department of Computer Science, SRM Institute of Science and Technology, Tamilnadu, India.

¹Corresponding Author : jayasreesrm@gmail.com

Received: 13 October 2024

Revised: 14 November 2024

Accepted: 12 December 2024

Published: 31 December 2024

Abstract - Tropical cyclone intensity classification is critical for disaster preparedness and resource allocation. Existing methods rely heavily on either manual analysis or computationally intensive deep learning models, which, despite their high accuracy, are often impractical for real-time scenarios. A significant gap exists in the literature where lightweight yet accurate models optimized for real-time applications are underexplored. This study addresses this gap by leveraging Gabor filter-based texture feature extraction combined with machine learning models, enabling precise cyclone intensity classification while balancing computational efficiency and prediction accuracy. By evaluating multiple classifiers, including Random Forest, SVM, and KNN, this study offers a comparative perspective to identify the most effective model for cyclone intensity classification in binary and multi-class setups.

Keywords - Tropical cyclone, Bayes Net, KNN, SVM, Intensity.

1. Introduction

Often accompanied by strong winds, heavy downpours of rain, and low atmospheric pressure, Tropical Cyclones (TCs) or typhoons are extreme meteorological events that may be catastrophic for affected coastal cities. For proper execution of preparedness and response strategies and to determine possible consequences of tropical storms, it is important to categorize the storms. In the past, conventions in defining TCs' genesis included factors like wind velocity and central pressure. Yet the complexity of these approaches makes it necessary to look at other complex approaches to classifying such events.

Usually, binary classification categorizes the TCs into two categories, "Tropical storm" and "Hurricane," but the multi-class classification allows for classification into several intensity classes. HHS has stated that tools like Support Vector Machines (SVM), K-Nearest Neighbors (KNN), Bayes Net, Random Forest, and Decision Trees Researchers can use such machine learning algorithms to automate the kind of categorization, improve the predicted accuracy and reduce the need for direct sifting through papers. However, there are feature extraction techniques that enhance the efficiency of these algorithms. For instance, Gabor wavelets are one of the most generally applied image analysis methods, which, if used in the feature extraction phase, can significantly enhance the TC intensity categorization accuracy.

Gabor filters are special for texture analysis and pattern recognition in images since they provide spatial and spatial frequency information. Given such studies, Gabor filters were defined to analyse complex satellite data using several frequency components to capture other structural aspects of tropical cyclones. Because cyclone strength has to be classified based on their differences, the ability to emphasize characteristics at different orientations and scales is critical because it allows for discerning small differences that correlate with the differences in intensity. It has been evidenced in previous studies that Gabor filters are quite effective for various applications, such as image recognition, medical image processing and analyzing complex natural phenomena such as the tropical cyclone.

However, literature research is still deficient in the comparative assessment of different machine learning strategies when combined with the Gabor filter. In contrast, the number of published papers on machine learning-based TC intensity categorization is gradually increasing. However, to the author's knowledge, no previous research has investigated how all these factors interact to produce outcomes in binary and multi-class classification systems.

To close this gap, it is vital to enhance the outcomes that define the approaches to accuracy enhancement of the TC intensity categorization, which is crucial in managing



disasters. The increase in intensity and frequency of tropical cyclones due to climate change is the fundamental motivation for the study. Scholars argue that the degree of TC intensity necessarily matters for enhancing forecasting, preparedness, and reaction to completion. In developing more accurate and automated categorization procedures, this study aims to contribute by looking at the Gabor filter and numerous machine learning methods. With higher levels of categorization, improved risk assessment and resource-allocating decisions could be achieved, and this might someday help save lives and minimize the monetary costs of these tropical cyclones.

The primary objective of this study is to determine the level of tropical cyclone strength differentiation initially as binary and then further as multi-class using Gabor filters on top of an assortment of machine learning algorithms, including SVM, KNN, BayesNet, Random Forest, Decision Trees, and so on. To identify whether the accuracies of TC intensity classification about different ratios of SH, GH, PS and other factors to be investigated in this study, the specific measures of performance of the various combinations shall be analyzed with careful calibrations. The results will provide valuable data to improve cyclone prediction and reduction knowledge, indicating that greater preparedness and reaction plans increase cyclone risk.

Current practices concerning cyclone intensity categorization can be grouped within a broad set of possibilities. Currently, many convolutional neural networks and long- and short-term memories are reported to produce high accuracy. For instance, Tian et al. (2024) applied spatiotemporal attention networks and got high accuracy in short-term intensity prediction. However, their methods require massive computations and are impractical for real-time use, especially in regions with limited resources. However, these traditional machine learning techniques, employed by Thenmozhi et al. (2024), sacrifice finer feature extraction necessary for intensity prediction for computational optimization.

This work links these approaches by incorporating Gabor filters, which were previously demonstrated to perform splendidly in capturing canonical texture-based inventions with lightweight classifiers like Random Forest. While similar in HLE accuracy to state-of-the-art deep learning models, these proposed results require far less computation. Unlike previous classifications that relied on classical filters, the novel addition of Gabor filters helps overcome an important drawback of previous studies in the differentiation between cyclone intensities.

This work is organized as follows: Section 2 presents a review of related research, Section 3 describes materials and techniques, Section 4 displays results and analysis, Section 5 concludes the work, and Section 5 describes the future scope.

2. Literature Survey

Tian et al. proposed STAC-Pred, a spatiotemporal attention convolutional network for real-time TC intensity prediction. The model improved performance by 0.47 and 0.28 compared to the interval at 3 and 6 hours, demonstrating significant improvements in short-term intensity prediction [1]. Ho et al. developed two AI models to determine TC centers in the western North Pacific: a CNN and an LSTM model. The models combined information from six networks of geostationary satellite imagery, demonstrating comparable or better performance than existing operational products [2].

Thenmozhi et al. utilized multi-criteria decision-making and ML models to assess cyclone risk and impact. The method assigned weights to various vulnerability criteria and employed SVM, SAM, and MLC algorithms to generate pre- and post-cyclone land use maps [3]. Choo et al. proposed a transfer learning approach with the Swin Transformer model for TC intensity estimation. The greatest pre-trained and TL models achieved deviations of 6.46 and 6.48 kts, showing 7% to 52% improvement over control models. This demonstrates the effectiveness of transfer learning in leveraging data from different satellite missions [4].

Sonet et al. used cloud-free satellite images and an SVM to examine land use and land shelter changes in pre- and post-cyclone phases to assess disaster impact. The study quantified land feature changes and flooding extent following Cyclone Bulbul in coastal Bangladesh [5]. Wang et al. introduced HuCL, a novel forecasting framework that integrates CNNs as well as LSTMs to progress and analyse multimodal data for TC track prediction. The model demonstrated improved accuracy in forecasting TC tracks in the Pacific Northwest compared to traditional unimodal methods [6]. Li et al. developed the “Time-based Attention Mechanism ConvLSTM” (TAM-CL) model for TC track and intensity prediction. The model uses ConvLSTM with 3D convolution kernels to enhance spatiotemporal feature extraction from atmospheric reanalysis data, incorporating an attention mechanism to advance long-term prediction outcomes [7].

Nasimi et al. proposed EESRGAN for automated estimation of tornado-induced treefall. The model achieved an accuracy up to 0.86 and an Average Precision (AP) of 0.88, demonstrating the potential of deep learning in post-disaster damage assessment [8]. Senior-Williams et al. evaluated transfer learning for tropical storm classification, with models achieving accuracies of 0.75, 0.82, 0.69, and 0.89 on four experimental datasets. These results demonstrate the potential of transfer learning in adapting pre-trained models to specialized meteorological tasks [9]. Patra et al. developed a satellite-based cyclone impact assessment methodology. The water and non-water pixel classification accuracy was 0.93 and 0.89 for pre- and post-images, respectively, demonstrating the approach's effectiveness in mapping cyclone-induced flooding [10].

Qian et al. reviewed recent advancements in TC governing and analysis techniques, focusing on climatological satellites, sensors, and aircraft. The study highlighted emerging technologies and products that support improved TC monitoring accuracy and operational capabilities [11]. Moustafa et al. proposed EESRGAN for cyclone detection in climate model data. The model attained an accuracy of up to 0.863 and a precision of 0.886, demonstrating the potential of super-resolution techniques in improving cyclone detection in low-resolution data [12]. Yao et al. developed a deep neural network approach for wind turbine load reduction during TCs. The load suppression effect was 1%-9% under different working conditions compared to traditional strategies, demonstrating the potential of ML in enhancing renewable energy infrastructure resilience [13]. May et al. demonstrated that a CNN based on the U-Net architecture can accurately identify clouds associated with tropical cyclones in geostationary infrared images [14]. Ma et al. developed DLPE-MST, a deep learning model for precipitation estimation from GOES-16 data. The algorithm outperformed others' POD and correlation, achieving scores of 0.91 and 0.58, respectively. These show the potential of deep learning in refining satellite-based precipitation estimates in TC conditions [15].

Juhyun Lee et al. developed a hybrid-CNN merging with the satellite imagery and statistical model outputs to forecast tropical cyclone intensity. This demonstrates the potential of deep learning approaches to substantially enhance TC intensity forecasting, particularly for challenging rapid intensification scenarios [16]. Wang et al. introduced a physics-novel improved deep CNN to determine centers of low-intensity tropical cyclones in satellite IR images. The model significantly improved accuracy over current-moment-only approaches by integrating consecutive images and historical TC information. Mean distance errors for tropical depression and tropical storm levels were reduced to 20.1 km and 19.1 km, representing improvements of 63.0% and 54.6%, respectively. This demonstrates the value of incorporating temporal information and physics-based knowledge into deep learning models for TC analysis [17]. Mu et al. developed the TC3R model for retrieving tropical cyclone rainfall information from C-band Sentinel-1 SAR imagery. When compared to SMAP measurements, it achieved an RMSE of 3.78 m/s. These results indicate that deep learning can extract rainfall information from SAR data, even in challenging TC conditions [18].

Kitamoto et al. presented the Digital Typhoon dataset, a 40+ year satellite image dataset for selected ML models on spatio-temporal tropical cyclone images. While not providing specific metrics, this dataset significantly contributes to the field, enabling more robust and comparable evaluations of TC analysis models [19]. Griffin et al. developed D-MINT and D-PRINT, two ML models to predict current and short-term intensity change in global typhoons. This suggests that

machine learning can complement and potentially enhance existing operational TC forecasting tools [20]. Zhao et al. proposed an effective TC tracking technique called SiamTCNet on DL with IR satellite images. It improves upon the SiamRPN network by incorporating spatiotemporal evolution characteristics and using multiple input frames to capture TC temporal changes [21].

Raynaud et al. introduced a U-Net based model to detect TC wind structure in outputs of the AROME model [22]. The model achieved 0.8 (average-intersection-over-union), demonstrating the potential of semantic segmentation approaches in TC wind field analysis [23]. Cui et al. developed an ML model and interpreted TC-induced sea surface temperature cooling spatial structure amplitude. It uses Extreme Gradient Boosting (XGBoost) with 12 TC and ocean state predictors, outperforming a numerical model in accuracy [24]. Pal et al. introduced Small Skip Net (SSN), a lightweight CNN-based architecture for classifying TC satellite images. The model got an overall accuracy (0.92) on the test set, demonstrating that efficient architectures can achieve high performance in TC classification tasks [25]. Bharathi et al. introduced a prophetic outline for typhoon prediction by SVM. The approach analyzes diverse climatological constraints to identify forms associated with cyclone growth, signifying robust acts in identifying potential cyclonal constructions [26]. Tian et al. proposed EasyRP-R-CNN, a convolutional-based cyclone detection framework focusing on improving efficiency. It introduces a new Region of Interest choice apparatus and a scale-based ROI consortium component to avoid classifying undersized ROIs [27].

Liu et al. introduced TCRainNet, a rainfall nowcasting model for TCs. The model's nowcasts had averaged POD and CSI greater than 0.27 and 0.2, respectively, with deviations below 2.6mm. These results demonstrate the model's ability to provide reasonably accurate short-term rainfall predictions for TCs [28]. Zhang et al. proposed the STIA model for TC intensity estimation using Himawari-8 satellite data. The model achieved an overall deviation of 3.61 m/s (RMSE) and 2.83 m/s (MAE), signifying strong performance in TC intensity assessment from geostationary IR images [29].

Li et al. introduced a transfer learning-based GAN framework for reconstructing inner-core high winds from SAR images during TC events. The model showed strong performance, with a bias of -0.69 m/s, deviation of 4.08 m/s, and R-value of 0.91 under heavy rainfall conditions, demonstrating the potential of GANs in improving SAR-based wind estimates in TCs [30].

Eusebi et al. developed a physics-informed neural network for TC data assimilation. This proposed model's ability to reconstruct realistic wind and pressure fields from sparse data demonstrates the potential of combining deep learning with physical constraints in TC analysis [31].

Hachiya et al. presented a novel practise for unfair ordinal multi-class classification of TC intensity changes. This approach addresses a common challenge in TC strength change prediction [32].

Mawatwal et al. proposed a hybrid architecture using a Convolutional Neural Network for automated cyclone intensity prediction. The model incorporates a binary, multi-class, YOLOv3-based cyclone indicator and deterioration module. It achieved high accuracy for binary classification ($98.4\% \pm 0.003$) and reasonable performance for multi-class classification ($63.83\% \pm 1.3$) and intensity estimation (RMSE of 16.2 ± 0.9 knots). These outcomes recommend that the hybrid approach can effectively handle different aspects of cyclone analysis, from detection to intensity estimation [33].

Nguyen and Kieu explored using ResNet and UNet architectures to predict tropical cyclone formation from large-scale environmental conditions. This proposed model showed the best performance at 12-18 hour forecast lead times and when using a vast area covering the Pacific Ocean. This suggests that CNNs can effectively capture the complex spatial patterns associated with TC formation, potentially improving early warning capabilities [34]. Tian et al. introduced TCIP-Net, a TC intensity prediction network that extracts convective structural information from IR satellite imagery. These models use Hovmöller diagrams to represent spatio-temporal evolution, and its subnetwork for capturing asymmetric TC structure information represents innovative approaches to TC intensity prediction [35].

Present-day approaches to cyclone intensity differentiation comprise a wide variety of classification techniques. A few recent studies on the architectures of deep learning models, such as CNNs and LSTMs, have very high accuracy rates. Tian et al. (2024) employed spatiotemporal attention networks to develop highly accurate short-term intensity prediction.

However, their methods require intensive computation to provide results, making them unsuitable for real-time applications in the scarcity of resources in the Third World. Computational models such as those employed by Thenmozhi et al. (2024) provide efficient machine learning but do not contain rich feature extraction required in intensity computations.

This work links these methodologies by presenting how Gabor filters, categorized for their ability to detect texture-based features, could be combined with simple classifiers such as Random Forest. While our approach is as accurate as actual deep learning models, our computational complexity is much lower. Compared with classical methods, introducing Gabor filters improves the capability to identify the difference in cyclone intensities, thus overcoming weaknesses in existing studies.

3. Materials and Methods

3.1. Description of the SINSAT3D Dataset

This research employs datasets of 136 infrared images extracted from the Kaggle repository featuring cyclone cases from 2012 to 2021 [36]. In the data preparation stage, images were resized to 224×224 pixels, converted to grayscale and then normalized. Further, image data was rotated and flipped to augment the dataset and improve the training of the models.

Normalization of filter responses was done by applying a combination of wavelet pyramid and statistical features of Gabor filters that turned out to be vital in extracting texture from cyclones. These features were used to train different machine learning classifiers: binary Random Forest, binary/Multi-class SVM, and binary/Multi-class KNN. Accuracy, recall, F1 score, and computational time offered a balanced parameter comparison.

3.1.1. Image Preprocessing

All images were converted to grayscale and resized to a uniform size to ensure consistency in the input data.

3.1.2. Gabor Filter

The Gabor filter was applied to extract image texture features.

The Gabor filter is defined as: $g(x_1, y_1; \lambda, \theta, \psi, \sigma, \gamma) = \exp(-(x_1^2 + \gamma^2 y_1^2) / (2\sigma^2)) * \cos(2\pi x_1 / \lambda + \psi)$.

- SVM: Performs well on high-dimensional data and is relatively immune from over-fitting when the right kernel is chosen.
- KNN: An easy-to-understand and applied method that is effective for low dimensional problems and delivers results without parameter estimation.
- Naive Bayes: Its applicability can, therefore, be analyzed as effective for data calibrated in binary or categorical terms according to probabilistic notions.
- Random Forest: An ensemble method used for accurate modeling and suitable for non-linear data.
- Decision Tree: An easily interpretable model with intuitive derivatives that can perform fast for small data sets.

3.1.3. Experimental Setup

The data was divided into 80% training and 20% testing set. Gabor filter features were used for binary classification with SVM, KNN and Naive Bayes, Decision Tree and Random Forest.

Random Forest and Decision Tree were applied for multi-class classification, and Gaussian filter features were used. The above models were carried out using the Python sklearn library. Different authors have defined training time differently, so the time taken to train each model was recorded.

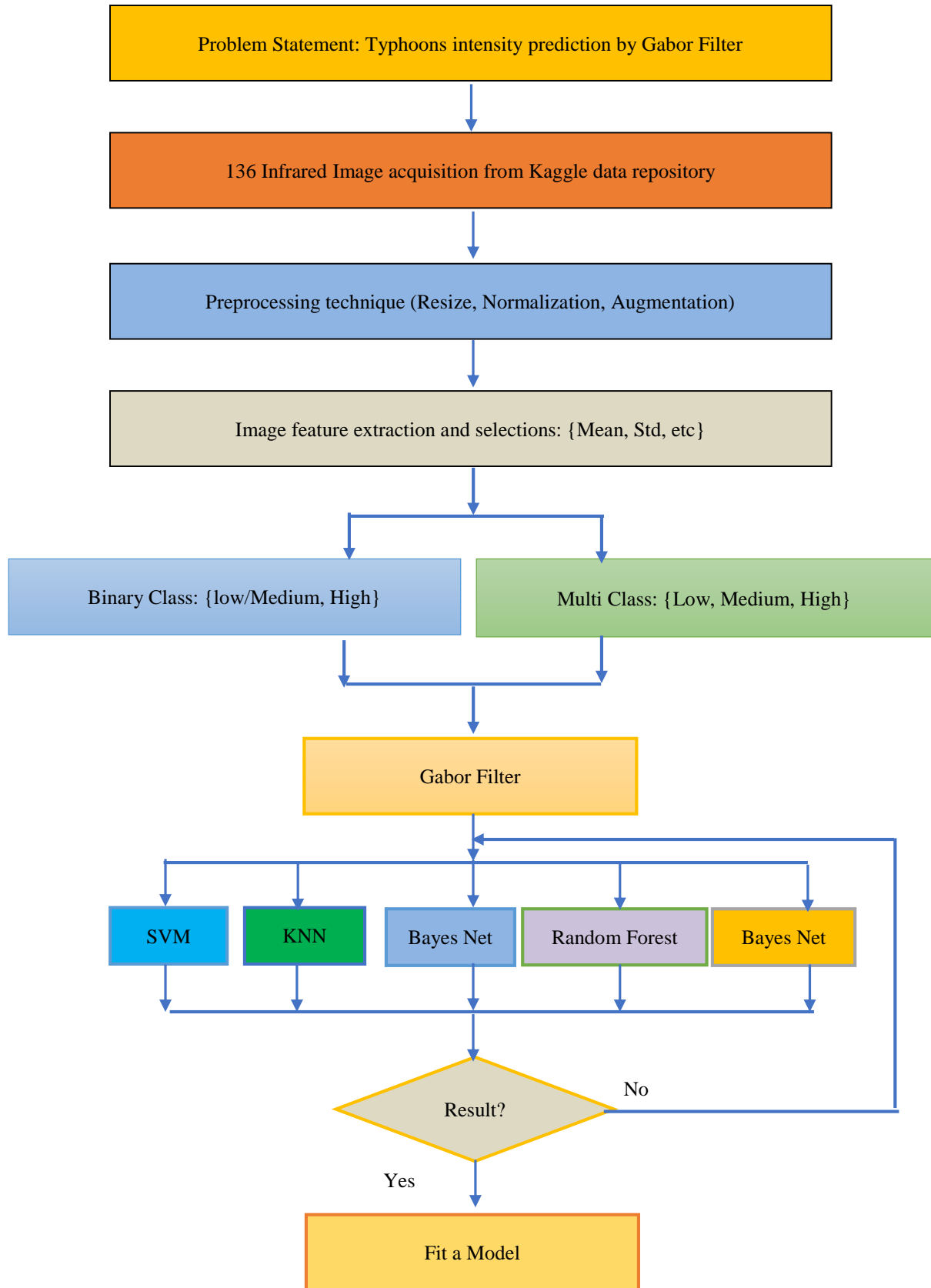


Fig. 1 Schema of the proposed system

Algorithm: Typhoon Intensity Classification using Multi-Feature Extraction and Ensemble ML (TICMFE-EML)

Input: Set of infrared satellite images $I = \{I_1, I_2, \dots, I_{136}\}$

Output: Typhoon intensity classification model M

Step 1 : Image Preprocessing: For each $I_i \in I$:

- a. Resize: $I_i^r = R(I_i, 224, 224)$, where R is the resize function
- b. Normalize: $I_i^n = (I_i^r - \min(I_i^r)) / (\max(I_i^r) - \min(I_i^r))$

Step 2 : Image Augmentation: For each I_i^n , generate:

- a. Flip: $I_i^f = F(I_i^n)$, where F is the flip function
- b. Rotate: $I_i^{\text{rot}} = \text{Rot}(I_i^n, \theta)$, where Rot is the rotation function and $\theta \in \{90^\circ, 180^\circ, 270^\circ\}$ Augmented set: $A = \{I_i^n, I_i^f, I_i^{\text{rot}}\}$ for all i , resulting in 3000 images

Step 3 : Feature Extraction: For each image $J \in A$, compute:

- a. Mean: $\mu = (1/N) \sum_{ij} J(i,j)$
- b. Std: $\sigma = \sqrt{((1/N) \sum_{ij} (J(i,j) - \mu)^2)}$
- c. Skewness: $\gamma_1 = E[(((X-\mu)/\sigma)^3)]$
- d. Kurtosis: $\gamma_2 = E[(((X-\mu)/\sigma)^4)] - 3$
- e. Entropy: $H = -\sum p(x) \log_2(p(x))$
- f. Eye Area: $A = \sum_{ij} E(i,j)$, where E is the binary eye region
- g. Eye Circularity: $C = 4\pi A / P^2$, where P is the perimeter of the eye
- h. Eye Eccentricity: $e = \sqrt{1 - (b^2/a^2)}$, where a and b are major and minor axes
- i. GLCM features: Compute contrast, homogeneity, energy, and correlation from GLCM matrix
- j. Gradient Mean: $\mu_{\text{grad}} = (1/N) \sum_{ij} |\nabla J(i,j)|$
- k. FFT Mean: $\mu_{\text{fft}} = (1/N) \sum_{uv} |F(u,v)|$, where F is the Fourier transform
- l. FFT STD: $\sigma_{\text{fft}} = \sqrt{((1/N) \sum_{uv} (|F(u,v)| - \mu_{\text{fft}})^2)}$

Step 4 : Feature Vector: For each image J , create feature vector: $X_J = [\mu, \sigma, \gamma_1, \gamma_2, H, A, C, e, \text{GLCM_features}, \mu_{\text{grad}}, \mu_{\text{fft}}, \sigma_{\text{fft}}]$

Step 5 : Classification Preparation:

- a. Binary: $Y_{\text{binary}} = \{0 \text{ if low/medium}, 1 \text{ if high}\}$
- b. Multi-class: $Y_{\text{multi}} = \{0 \text{ if low}, 1 \text{ if medium}, 2 \text{ if high}\}$
- c. Balance dataset: Randomly select 300 images for each class

Step 6 : Filtering: Gabor Filter: $g(x_1, y_1; \lambda, \theta, \psi, \sigma, \gamma) = \exp(-(x_1^2 + \gamma^2 y_1^2) / (2\sigma^2)) \cos(2\pi x_1 / \lambda + \psi)$

Where $x' = x \cos \theta + y \sin \theta$, $y' = -x \sin \theta + y \cos \theta$ $J_{\text{Gab}} = J * g$

Step 7 : Machine Learning Models:

- a. SVM: $f(x) = \text{sign}(w^T x + b)$
- b. KNN: $y = \text{mode}(y_i)$ for k nearest neighbors
- c. Naive Bayes: $P(y|x) = P(x|y)P(y) / P(x)$
- d. Random Forest: $y = \text{mode}(\text{tree}_i(x))$ for $i=1$ to n_{trees}
- e. Decision Tree: $y = \text{leaf_value}(x)$

Step 8 : Model Evaluation: For each model m :

- a. Accuracy: Acc_m
- b. Precision: Prec_m
- c. Recall: Rec_m
- d. F1 Score: F1_m , etc

Step 9 : Model Selection and Fitting: $M = \text{argmax}_m (\text{F1}_m)$
Train M on entire dataset

Figure 1 shows the following methods for predicting an optimal outcome using the ML models.

4. Results and Discussion

This section focuses on the results and discussions of the binary class and multi class classification with Gabor filter by SVM, KNN, Bayes Net, Decision Tree, and Random Tree for predicting the intensity of tropical cyclones of infrared images.

Table 1 presents the accuracy metrics for various classifiers applied to binary and multi-class classification tasks. The Binary Class SVM and Multi Class SVM both achieve an accuracy of 0.79, indicating consistent performance across classification types. The Binary Class KNN has an accuracy of 0.75, while the Multi Class KNN performs slightly better at 0.78. The Binary Class Bayes Net achieves an accuracy of 0.78, closely followed by the Multi Class Bayes Net at 0.77. The Binary Class Random Forest classifier excels with the highest accuracy of 0.88, and the Multi Class Random Forest also demonstrates strong performance with an accuracy of 0.86. The Binary Class Decision Tree records an accuracy of 0.81, while the Multi Class Decision Tree has a lower accuracy of 0.73. Overall, the Random Forest classifiers stand out in accuracy, while SVM and KNN classifiers display comparable effectiveness in binary and multi-class settings.

Table 1 outlines the precision metrics for various classifiers in binary and multi-class classification scenarios. The Binary Class SVM and Multi Class SVM maintain a precision score of 0.79, demonstrating consistent effectiveness in identifying relevant instances. The Binary Class KNN exhibits a precision of 0.75, while the Multi Class KNN slightly outperforms it with a precision of 0.78. Both the Binary Class Bayes Net and Multi Class Bayes Net classifiers achieve a precision of 0.77, indicating a balanced performance across both classification types. The Binary Class Random Forest achieves the highest precision at 0.88, while the Multi Class Random Forest also performs strongly at 0.86. Meanwhile, the Binary Class Decision Tree records a precision of 0.81, while the Multi Class Decision Tree shows a lower precision of 0.73. In summary, Random Forest classifiers demonstrate superior precision, while SVM and KNN classifiers exhibit competitive results across both classification types.

Table 1 presents the recall metrics for various classifiers in binary and multi-class classification tasks. The Binary Class SVM and Multi Class SVM achieve identical recall scores of 0.79, reflecting a strong capability to identify relevant instances across both classification scenarios. In contrast, the

Binary Class KNN shows a lower recall of 0.53, and the Multi Class KNN further decreases to 0.36, indicating a struggle to capture positive instances effectively. The Binary Class Bayes Net exhibits a recall of 0.58, while the Multi Class Bayes Net maintains a slightly lower recall at 0.53. Notably, the Binary Class Random Forest and Multi Class Random Forest classifiers excel in the recall, with scores of 0.88 and 0.86, respectively, demonstrating their strong performance in identifying true positives. The Binary Class Decision Tree also performs well, with a recall of 0.81, while the Multi Class Decision Tree has a lower recall of 0.73. Overall, Random Forest classifiers stand out in recall performance, whereas KNN classifiers show challenges in capturing relevant instances effectively.

Table 1 outlines the Receiver Operating Characteristic (ROC) scores for various classifiers in binary, multi-class classification tasks. The Binary Class SVM achieves an ROC score of 0.88, while the Multi Class SVM performs even better with an ROC of 0.94, indicating strong discriminatory ability between classes. In contrast, the Binary Class KNN and Multi Class KNN show lower ROC scores of 0.67 and 0.75, respectively, suggesting less effective classification performance. The Binary Class Bayes Net has a notably low ROC of 0.60, with the Multi Class Bayes Net improving slightly to 0.67, indicating limited capability in distinguishing between classes. Both Random Forest classifiers stand out with high ROC scores: 0.95 for the Binary Class Random Forest and 0.96 for the Multi Class Random Forest, reflecting their excellent classification performance. Lastly, the Binary Class Decision Tree shows an ROC of 0.81, while the Multi Class Decision Tree slightly drops to 0.80, indicating good, though not exceptional, performance in class differentiation. Overall, Random Forest and SVM classifiers demonstrate superior ROC scores, indicating their robustness in multi-class and binary classification tasks.

Table 1 presents the Precision-Recall Curve (PRC) scores for various classifiers in binary, multi-class classification tasks. The Binary Class SVM achieves a high PRC score of 0.90, while the Multi Class SVM slightly improves to 0.92, indicating effective precision in identifying positive instances across multiple classes. In contrast, both KNN classifiers perform notably lower, with the Binary Class KNN at 0.66 and the Multi Class KNN at 0.61, suggesting challenges in maintaining precision. The performance of the Bayes Net classifiers is also limited, with the Binary Class Bayes Net scoring 0.54 and the Multi Class Bayes Net at 0.50, reflecting a decrease in precision. Both Random Forest classifiers excel, achieving scores of 0.94 for the Binary Class Random Forest and 0.95 for the Multi Class Random Forest, demonstrating outstanding precision in predicting positive cases. Lastly, the Binary Class Decision Tree scores 0.81, while the Multi Class Decision Tree lags at 0.62, indicating varying precision levels. The Random Forest and SVM classifiers showcase the

strongest PRC scores, highlighting their reliability in multi-class and binary classification tasks.

Table 1 has F-Measure results for the various classifiers that illustrate their effectiveness in balancing precision and recall across binary and multi-class classification tasks. The Binary and Multi Class SVM achieve an F-Measure of 0.79, indicating consistent performance in accurately classifying instances in both scenarios. In contrast, the Binary Class KNN and Multi Class KNN show considerably lower F-Measure scores of 0.39 and 0.22, respectively, suggesting that KNN struggles to balance precision and recall, particularly in multi-class situations. The Binary Class Bayes Net achieves an F-Measure of 0.51, while the Multi Class Bayes Net slightly improves to 0.52, reflecting moderate performance but still below optimal levels. The Random Forest classifiers excel, with the Binary Class Random Forest scoring 0.88 and the Multi Class Random Forest at 0.86, indicating a strong ability to balance precision and recall across both types of classification. Lastly, the Decision Tree classifiers show solid results, scoring 0.81 for binary classification and 0.73 for multi-class classification, demonstrating robust performance though slightly less effective than Random Forest in multi-class scenarios.

The MCC scores for the classifiers indicate their effectiveness in handling binary and multi-class classification tasks. The Binary Class SVM achieves an MCC of 0.58. At the same time, the Multi Class SVM demonstrates improved performance with an MCC of 0.68, suggesting that the SVM models effectively provide a balanced representation of true and predicted classifications. In contrast, the Binary Class KNN and Multi Class KNN yield low MCC scores of 0.13 and 0.14, respectively, indicating their struggle to classify instances accurately and reflect the actual distribution of classes. The Binary Class Bayes Net scores 0.32, and the Multi Class Bayes Net improves slightly to 0.42, highlighting moderate performance but still showing room for improvement. The Random Forest classifiers stand out with impressive MCC scores of 0.77 for the binary classification and 0.79 for multi-class classification, signifying their robustness in accurately capturing the correlation between actual and predicted values. Lastly, the Binary Class Decision Tree achieves an MCC of 0.62, while the Multi Class Decision Tree scores 0.59, indicating reasonable performance but not as strong as the Random Forest models.

The Kappa statistics for the classifiers provide insights into their agreement with the true class labels beyond chance. For the Binary Class SVM, the Kappa value is 0.58; for the Multi Class SVM, it is 0.68, indicating moderate agreement and suggesting that these models perform better than random guessing. In contrast, the Binary Class KNN and Multi Class KNN show very low Kappa values of 0.04, reflecting poor agreement with the true labels and indicating that these classifiers are not effectively distinguishing between classes.

The Binary Class Bayes Net scores 0.18, while the Multi Class Bayes Net slightly improves with 0.32, indicating minimal agreement. The Binary Class Random Forest excels with a Kappa value of 0.77, and the Multi Class Random Forest also performs strongly with 0.79, indicating substantial agreement with the true classifications. Finally, the Binary Class Decision Tree has a Kappa value of 0.62, and the Multi Class Decision Tree scores 0.59, reflecting reasonable agreement but not as robust as the Random Forest models. The MAE values measure the average absolute errors between predicted and actual values, reflecting the accuracy of the classifiers in binary and multi-class settings. For the Binary Class SVM, the MAE is 0.21, while the Multi Class SVM shows a slightly higher error of 0.28, indicating reasonable performance in both classifications. The Binary Class KNN has a higher MAE of 0.47, and the Multi Class KNN exhibits a significant increase to 0.92, suggesting that the KNN models are less effective at making accurate predictions. The Binary Class Bayes Net records an MAE of 0.42, and the Multi Class Bayes Net has a higher MAE of 0.67, indicating a moderate error level.

In contrast, the Binary Class Random Forest performs exceptionally well with the lowest MAE of 0.12, followed by the Multi Class Random Forest with an MAE of 0.16,

demonstrating its effectiveness in making accurate predictions. Lastly, the Binary Class Decision Tree has an MAE of 0.19. At the same time, the Multi Class Decision Tree shows an MAE of 0.34, indicating that decision trees have moderate predictive capabilities compared to the Random Forest models. The RMSE values quantify the differences between predicted and actual outcomes, with lower values indicating better predictive accuracy. For the Binary Class SVM, the RMSE is 0.46, while the Multi Class SVM shows a higher RMSE of 0.64, suggesting that the multi-class model has a more significant average error. The Binary Class KNN has an RMSE of 0.68, which increases significantly to 1.23 for the Multi Class KNN, indicating a substantial drop in predictive performance for multi-class scenarios. Similarly, the Binary Class Bayes Net exhibits an RMSE of 0.65, while the Multi Class Bayes Net has an even higher RMSE of 1.04, further reflecting the challenges in multi-class predictions. The Binary Class Random Forest demonstrates strong performance with the lowest RMSE of 0.34, while the Multi Class Random Forest has a slightly higher RMSE of 0.45 but remains competitive. The Binary Class Decision Tree shows an RMSE of 0.44. At the same time, the Multi Class Decision Tree has an RMSE of 0.69, indicating that decision trees also perform reasonably well but do not match the Random Forest models. Overall, the Random Forest classifiers again emerge as the most reliable models with the lowest RMSE values across binary and multi-class classifications, emphasizing their robustness in predicting outcomes.

Table 1. Binary and multi class with Gabor filter by ML models vs. Classification metrics

Sl. No	Classifier	Accuracy	Precision	Recall	ROC	PRC	Kappa	F1-Score	MCC	MAE	RRSE	RAE	RRSE	Time
1	Binary Class + SVM	0.79	0.79	0.79	0.88	0.9	0.58	0.79	0.58	0.21	0.46	0.42	0.91	25.73
2	Multi Class + SVM	0.79	0.79	0.79	0.94	0.92	0.68	0.79	0.68	0.28	0.64	0.43	0.81	79.79
3	Binary Class + KNN	0.75	0.75	0.53	0.67	0.66	0.04	0.39	0.13	0.47	0.68	0.93	1.37	0
4	Multi Class + KNN	0.78	0.78	0.36	0.75	0.61	0.04	0.22	0.14	0.92	1.23	1.45	1.55	0
5	Binary Class + Bayes Net	0.78	0.77	0.58	0.6	0.54	0.18	0.51	0.32	0.42	0.65	0.83	1.29	0.22
6	Multi Class + Bayes Net	0.77	0.77	0.53	0.67	0.5	0.32	0.52	0.42	0.67	1.04	1.04	1.32	0.36
7	Binary Class + Random Forest	0.88	0.88	0.88	0.95	0.94	0.77	0.88	0.77	0.12	0.34	0.23	0.68	1.46
8	Multi Class + Random Forest	0.86	0.86	0.86	0.96	0.95	0.79	0.86	0.79	0.16	0.45	0.25	0.57	2.96
9	Binary Class + Decision Tree	0.81	0.81	0.81	0.81	0.81	0.62	0.81	0.62	0.19	0.44	0.38	0.88	3.19
10	Multi Class + Decision Tree	0.73	0.73	0.73	0.8	0.62	0.59	0.73	0.59	0.34	0.69	0.53	0.87	7.14

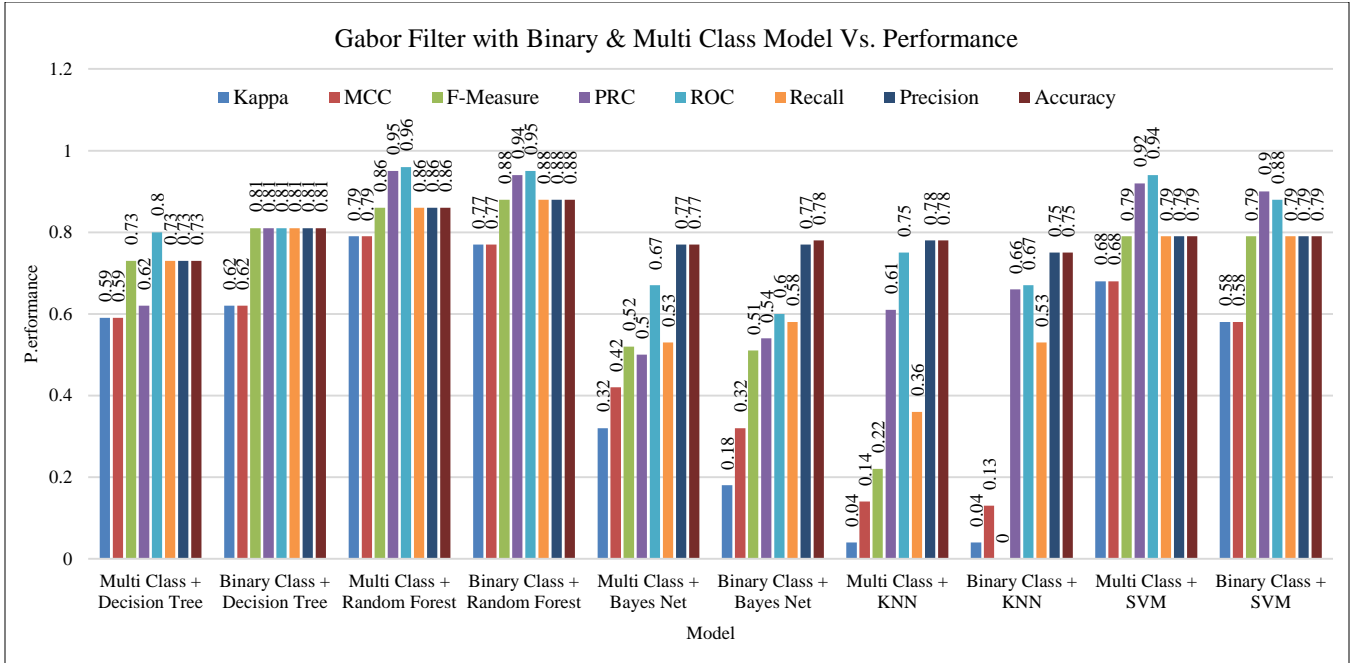


Fig. 2 Binary and multi class with Gabor filter by ML models Vs. Classification metrics



Fig. 3 Binary and multi class with Gabor filter by ML models Vs. Regression metrics

The Relative Absolute Error (RAE) measures the accuracy of predictions by comparing the absolute error to a baseline, with lower values indicating better performance. For the Binary Class SVM, the RAE is 0.42. At the same time, the Multi Class SVM shows a marginally higher RAE of 0.43, suggesting that the performance in binary and multi-class scenarios is quite similar. The Binary Class KNN has a significantly higher RAE of 0.93, which increases to 1.45 for the Multi Class KNN, indicating a substantial deterioration in

prediction accuracy for the multi-class setting. Similarly, the Binary Class Bayes Net has an RAE of 0.83, which escalates to 1.04 for the Multi Class Bayes Net, reflecting the increased difficulty of multi-class predictions. In contrast, the Binary Class Random Forest performs best with the lowest RAE of 0.23, while the Multi Class Random Forest has a slightly higher RAE of 0.25 yet still indicates strong predictive capabilities.

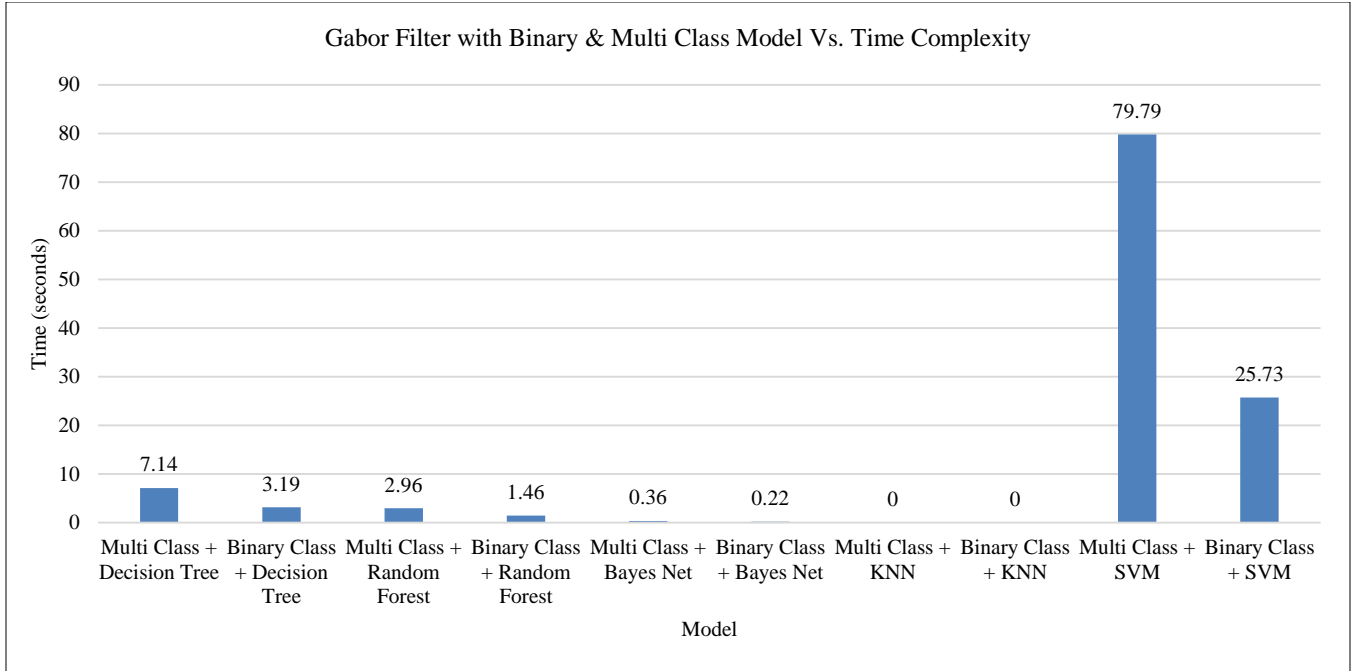


Fig. 4 Binary and multi class with Gabor filter by ML models Vs. Time complexity

Lastly, the Binary Class Decision Tree has an RAE of 0.38. At the same time, the Multi Class Decision Tree rises to 0.53, highlighting a similar trend where decision trees also perform less effectively in multi-class situations. Overall, Random Forest models continue to demonstrate superior performance across both binary and multi-class classifications, evidenced by their lower relative absolute error values.

The Root Relative Squared Error (RRSE) quantifies the prediction error relative to the magnitude of the observed values, with lower values indicating better predictive performance. For the Binary Class SVM, the RRSE is 0.91, suggesting a moderate error in predictions. In contrast, the Multi Class SVM shows improved performance with an RRSE of 0.81, indicating that it is more accurate in a multi-class scenario than the binary classification. The Binary Class KNN has a significantly higher RRSE of 1.37, which further increases to 1.55 for the Multi Class KNN, demonstrating a notable decline in prediction accuracy in the multi-class case. The Binary Class Bayes Net records an RRSE of 1.29. At the same time, the Multi Class Bayes Net exhibits a slightly higher value of 1.32, reflecting similar performance across both classification types but with considerable error. The Binary Class Random Forest stands out with the lowest RRSE of 0.68, and the Multi Class Random Forest further improves this performance with an RRSE of 0.57, indicating strong predictive accuracy in both scenarios. Lastly, the Binary Class Decision Tree shows an RRSE of 0.88, and the Multi Class Decision Tree has a marginally lower value of 0.87, suggesting a stable but less impressive performance compared to the Random Forest models.

The time complexity for various classifiers indicates the computational resources required for processing data and making predictions. For Binary Class SVM, the time complexity is 25.73 seconds, while the Multi Class SVM significantly increases to 79.79 seconds, demonstrating a higher demand for computation in multi-class scenarios. In contrast, both Binary Class KNN and Multi Class KNN have a time complexity of 0 seconds, suggesting that they are speedy, likely due to their instance-based learning approach. The Binary Class Bayes Net takes 0.22 seconds, and the Multi Class Bayes Net takes 0.36 seconds, indicating efficient performance in both cases.

The Binary Class Random Forest shows a time complexity of 1.46 seconds, which increases to 2.96 seconds for the Multi Class Random Forest, reflecting a moderate increase in computational time for multi-class classification. The Binary Class Decision Tree requires 3.19 seconds. In comparison, the Multi Class Decision Tree increases this to 7.14 seconds, indicating that decision trees, while still relatively quick, take more time as the complexity of the task increases. KNN classifiers exhibit the least time complexity, while SVM models demand the most computational resources, particularly in multi-class situations.

4.1. Classifier Performance

Random Forest was the most accurate model in all the aspects of binary classification, with an accuracy of 0.88 and multi class classification, with an accuracy of 0.86. SVM achieved a competitive accuracy of 0.79. However, it was considerably slower regarding computational time (79.79s) when performing multi-class classification. KNN proved fast

and efficient with processing times being measured in near-instances and was the model with the least recall of 0.36, especially when tested in a multi-class environment. The findings underpin the recommendation that Random Forest is the most effective algorithm for real-time applications since it provides reasonable accuracy and uses limited computational resources.

4.2. Computational Efficiency in Relation to Prediction Accuracy

As seen in this study, there is always a compromise between the time the algorithm takes to make a prediction and the prediction accuracy. Although SVM offers good accuracy here, it was several times slower than the other algorithms, making it unfit for real-time use. However, as seen in Figure 4, KNN had a minimum computational time but low accuracy and recall, and it would not be suitable for use in important operations. Random Forest learned that high accuracy could easily be achieved with relatively average computational resources, thus making it possible to implement it in disaster management cases where timeliness is vital.

4.3. Possibilities in Practical Cases

In real-world applications such as evacuation planning and resource estimation, the speed of the solution and the degree of precision required are important considerations. Based on the results, Random Forest can be recommended for deploying real-time applications because its accuracy is acceptably high and time-consuming is reasonable (approximately 2.96 seconds in multi-class classification task). This capability is especially useful in areas of the world

with limited high-performance computing resources, a factor that can prove expensive in many cases.

4.4. Comparison of the Proposed with Existing Work

Thus, compared to the deep learning models that Juhyun Lee et al. propose (2024), the proposed approach performs almost as effectively but consumes much less computational resources. This makes it a viable alternative for regions with limited computational capacity aside from the reduction in response time experienced by models trained on this framework. Moreover, the Gabor filters give a head start compared to the conventional machine learning models because they offer better feature extraction and, thus, better classification results.

5. Conclusion

This research shows the utility of an ensemble of Gabor filters and machine learning models for TC intensity prediction. Compared to all the other classifiers, Random Forest securely took the highest accuracy mark, with 0.88 in binary classification and 0.86 in multi-class classification. However, computational time usage was not significantly high.

The research fills the gap between developing highly accurate deep learning models and using computationally efficient algorithms for applications requiring real-time information processing. Further work could be done to study the Gabor filters in conjunction with deep learning approaches to improve the measure's efficiency.

References

- [1] Wei Tian et al., "Predicting the Intensity of Tropical Cyclones Over the Western North Pacific Using a Dual-Branch Spatiotemporal Attention Convolutional Network," *Weather and Forecasting*, vol. 39, no. 5, pp. 807-819, 2024. [[CrossRef](#)] [[Google Scholar](#)] [[Publisher Link](#)]
- [2] Chang-Hoi Ho et al., "Geostationary Satellite-Derived Positioning of a Tropical Cyclone Center Using Artificial Intelligence Algorithms Over the Western North Pacific," *Bulletin of the American Meteorological Society*, vol.105, no. 3, pp. E486-E500, 2024. [[CrossRef](#)] [[Google Scholar](#)] [[Publisher Link](#)]
- [3] M. Thenmozhi et al., "Assessment of Cyclone Risk and Case Study of Gaja Cyclone Using GIS Techniques and Machine Learning Algorithms in Coastal Zone of Tamil Nadu, India," *Environmental Research*, vol. 246, 2024. [[CrossRef](#)] [[Google Scholar](#)] [[Publisher Link](#)]
- [4] Minki Choo et al., "Bridging Satellite Missions: Deep Transfer Learning for Enhanced Tropical Cyclone Intensity Estimation," *GIScience & Remote Sensing*, vol. 61, no. 1,2024. [[CrossRef](#)] [[Google Scholar](#)] [[Publisher Link](#)]
- [5] M. Shahriar Sonet et al., "Assessing Tropical Cyclone Impacts in Coastal Bangladesh: A Change Detection Analysis on Cyclone Bulbul Using Geospatial Analysis and Remote Sensing Techniques," *International Journal of Disaster Risk Reduction*, vol. 112, 2024. [[CrossRef](#)] [[Google Scholar](#)] [[Publisher Link](#)]
- [6] Wennan Wang et al., "A Multimodal Deep Learning Approach for Hurricane Tack Forecast Based on Encoder-Decoder Framework," *Pattern Analysis and Applications*, vol. 27, no. 4, pp. 1-6, 2024. [[CrossRef](#)] [[Google Scholar](#)] [[Publisher Link](#)]
- [7] Tongfei Li et al., "Tropical Cyclone Trajectory Based on Satellite Remote Sensing Prediction and Time Attention Mechanism ConvLSTM Model," *Big Data Research*, vol. 36, 2024. [[CrossRef](#)] [[Google Scholar](#)] [[Publisher Link](#)]
- [8] Mitra Nasimi, and Richard L. Wood, "Using Deep Learning and Advanced Image Processing for the Automated Estimation of Tornado-Induced Treefall," *Remote Sensing*, vol. 16, no. 7, pp. 1-22, 2024. [[CrossRef](#)] [[Google Scholar](#)] [[Publisher Link](#)]

- [9] Jacob Senior-Williams et al., "The Classification of Tropical Storm Systems in Infrared Geostationary Weather Satellite Images Using Transfer Learning," *IEEE Journal of Selected Topics in Applied Earth Observations and Remote Sensing*, vol. 17, pp. 5234-5244, 2024. [[CrossRef](#)] [[Google Scholar](#)] [[Publisher Link](#)]
- [10] Prachee Patra, Umakanta Das, and Sonam Agrawal, "Satellite Imagery-Based Tropical Cyclone Impact Assessment on LULC and Vegetation: A Case Study of Cyclone Biparjoy," *Environmental Monitoring and Assessment*, vol. 196, 2024. [[CrossRef](#)] [[Google Scholar](#)] [[Publisher Link](#)]
- [11] Chuanhai Qian et al., "Tropical Cyclone Monitoring and Analysis Techniques: A Review," *Journal of Meteorological Research*, vol. 8, pp. 351-367, 2024. [[CrossRef](#)] [[Google Scholar](#)] [[Publisher Link](#)]
- [12] Marwa S. Moustafa et al., "Cyclone Detection with End-to-End Super Resolution and Faster R-CNN," *Earth Science Informatics*, vol. 17, pp. 1837-1850, 2024. [[CrossRef](#)] [[Google Scholar](#)] [[Publisher Link](#)]
- [13] Qi Yao et al., "Anti-Tropical Cyclone Load Reduction Control of Wind Turbines Based on Deep Neural Network Yaw Algorithm," *Applied Energy*, vol. 376, 2024. [[CrossRef](#)] [[Google Scholar](#)] [[Publisher Link](#)]
- [14] Joshua May et al., "Automated Segmentation of Tropical Cyclone Clouds in Geostationary Infrared Images," *IEEE Geoscience and Remote Sensing Letters*, vol. 21, 2024. [[CrossRef](#)] [[Google Scholar](#)] [[Publisher Link](#)]
- [15] Guangyi Ma et al., "An Improved Deep-Learning-Based Precipitation Estimation Algorithm Using Multitemporal GOES-16 Images," *IEEE Transactions on Geoscience and Remote Sensing*, vol. 62, pp. 1-17, 2024. [[CrossRef](#)] [[Google Scholar](#)] [[Publisher Link](#)]
- [16] Juhyun Lee, Junggho Im, and Yeji Shin, "Enhancing Tropical Cyclone Intensity Forecasting with Explainable Deep Learning Integrating Satellite Observations and Numerical Model Outputs," *50 iScience*, vol. 27, no. 6, 2024. [[CrossRef](#)] [[Google Scholar](#)] [[Publisher Link](#)]
- [17] Han Wang et al., "Determination of Low-Intensity Tropical Cyclone Centers in Geostationary Satellite Images Using a Physics-Enhanced Deep-Learning Model," *IEEE Transactions on Geoscience and Remote Sensing*, vol. 62, pp. 1-10, 2024. [[CrossRef](#)] [[Google Scholar](#)] [[Publisher Link](#)]
- [18] Shanshan Mu et al., "High-Resolution Tropical Cyclone Rainfall Detection From C-Band SAR Imagery with Deep Learning," *IEEE Transactions on Geoscience and Remote Sensing*, vol. 62, pp. 1-15, 2024. [[CrossRef](#)] [[Google Scholar](#)] [[Publisher Link](#)]
- [19] Asanobu Kitamoto et al., "Digital Typhoon: Long-Term Satellite Image Dataset for the Spatio-Temporal Modeling of Tropical Cyclones," *37th Conference on Neural Information Processing Systems (NeurIPS)*, vol. 36, pp. 40623-40636, 2024. [[Google Scholar](#)] [[Publisher Link](#)]
- [20] Sarah M. Griffin, Anthony Wimmers, and Christopher S. Velden, "Predicting Short-Term Intensity Change in Tropical Cyclones Using a Convolutional Neural Network," *Weather and Forecasting*, vol. 39, no. 1, pp. 177-202, 2024. [[CrossRef](#)] [[Google Scholar](#)] [[Publisher Link](#)]
- [21] Chang-Jiang Zhang et al., "Tropical Cyclone Tracking from Geostationary Infrared Satellite Images using Deep learning Techniques," *International Journal of Remote Sensing*, vol. 45, no. 18, pp. 6324-6341, 2024. [[CrossRef](#)] [[Google Scholar](#)] [[Publisher Link](#)]
- [22] Zhitao Zhao et al., "MT-GN: Multi-Task-Learning-Based Graph Residual Network for Tropical Cyclone Intensity Estimation," *Remote Sensing*, vol. 16, no. 2, pp. 1-22, 2024. [[CrossRef](#)] [[Google Scholar](#)] [[Publisher Link](#)]
- [23] L. Raynaud et al., "A Convolutional Neural Network for Tropical Cyclone Wind Structure Identification in Kilometer-Scale Forecasts," *Artificial Intelligence for the Earth Systems*, vol. 3, no. 2, pp. 1-15, 2024. [[CrossRef](#)] [[Google Scholar](#)] [[Publisher Link](#)]
- [24] Hongxing Cui et al., "Modeling Ocean Cooling Induced by Tropical Cyclone Wind Pump Using Explainable Machine Learning Framework," *IEEE Transactions on Geoscience and Remote Sensing*, vol. 62, pp. 1-17, 2024. [[CrossRef](#)] [[Google Scholar](#)] [[Publisher Link](#)]
- [25] Soumyajit Pal, Uma Das, and Oishila Bandyopadhyay, "SSN: A Novel CNN-Based Architecture for Classification of Tropical Cyclone Images From INSAT-3D," *IEEE Transactions on Geoscience and Remote Sensing*, vol. 62, pp. 1-8, 2024. [[CrossRef](#)] [[Google Scholar](#)] [[Publisher Link](#)]
- [26] K. Bharathi, A. Archita, and S. Gandhimathi Alias Usha, *Predicting Tropical Cyclones: A Supervised Machine Learning Approach*, Predicting Natural Disasters with AI and Machine Learning, IGI Global, pp. 158-172, 2024. [[CrossRef](#)] [[Google Scholar](#)] [[Publisher Link](#)]
- [27] Xiaoxian Tian et al., "EasyRP-R-CNN: a Fast Cyclone Detection Model," *The Visual Computer*, vol. 40, pp. 4829-4841, 2024. [[CrossRef](#)] [[Google Scholar](#)] [[Publisher Link](#)]
- [28] Li Liu et al., "Enhanced Rainfall Nowcasting of Tropical Cyclone by an Interpretable Deep Learning Model and Its Application in Real-time Flood Forecasting," *Journal of Hydrology*, vol. 644, 2024. [[CrossRef](#)] [[Google Scholar](#)] [[Publisher Link](#)]
- [29] Rui Zhang et al., "Estimating Tropical Cyclone Intensity Using an STIA Model FROM Himawari-8 Satellite Images in the Western North Pacific Basin," *IEEE Transactions on Geoscience and Remote Sensing*, vol. 62, pp. 1-13, 2024. [[CrossRef](#)] [[Google Scholar](#)] [[Publisher Link](#)]
- [30] Xiaohui L et al., "Transfer Learning-Based Generative Adversarial Network Model for Tropical Cyclone Wind Speed Reconstruction from SAR Images," *IEEE Transactions on Geoscience and Remote Sensing*, vol. 62, pp. 1-16, 2024. [[CrossRef](#)] [[Google Scholar](#)] [[Publisher Link](#)]

- [31] Ryan Eusebi et al., "Realistic Tropical Cyclone Wind and Pressure Fields Can Be Reconstructed from Sparse Data Using Deep Learning," *Communications Earth & Environment*, vol. 5, no. 8, pp. 1-10, 2024. [[CrossRef](#)] [[Google Scholar](#)] [[Publisher Link](#)]
- [32] Hirotaka Hachiya et al., "Multi-Class AUC Maximization for Imbalanced Ordinal Multi-Stage Tropical Cyclone Intensity Change Forecast," *Machine Learning with Applications*, vol. 17, 2024. [[CrossRef](#)] [[Google Scholar](#)] [[Publisher Link](#)]
- [33] Manish Kumar Mawatwal, and Saurabh Das, "An End-to-End Deep Learning Framework for Cyclone Intensity Estimation in North Indian Ocean Region Using Satellite Imagery," *Journal of the Indian Society of Remote Sensing*, vol. 52, pp. 2165-2175, 2024. [[CrossRef](#)] [[Google Scholar](#)] [[Publisher Link](#)]
- [34] Quan Nguye, and Chanh Kieu, "Predicting Tropical Cyclone Formation with Deep Learning," *Weather and Forecasting*, vol. 39, no. 1, pp. 241-258, 2024. [[CrossRef](#)] [[Google Scholar](#)] [[Publisher Link](#)]
- [35] Wei Tian et al., "TCIP-Net: Quantifying Radial Structure Evolution for Tropical Cyclone Intensity Prediction," *IEEE Transactions on Geoscience and Remote Sensing*, vol. 62, pp. 1-14, 2024. [[CrossRef](#)] [[Google Scholar](#)] [[Publisher Link](#)]
- [36] Sshubam Verma, INSAT3D Infrared and Raw Cyclone Imagery (2012-2021), Kaggle, 2021. [Online]. Available: <https://www.kaggle.com/datasets/sshubam/insat3d-infrared-raw-cyclone-images-20132021>